UPWIND SAIL AERODYNAMICS: A PRESSURE DISTRIBUTION DATABASE FOR THE VALIDATION OF NUMERICAL CODES

I M Viola, School of Marine Science and Technology, Newcastle University, UK
J Pilate and R G J Flay, Yacht Research Unit, The University of Auckland, New Zealand
(DOI No: XXX)

SUMMARY

The present paper aims to provide a benchmark set of sail pressure distributions for the validation of numerical codes. Modern upwind sails were built at 1/15th-scale and tested in a wind tunnel. The sails were built as a fibreglass sandwich and the pressures were transmitted through channels inside the core. The sails were supported with wind-transparent fishing lines, and a flat plate was used to model the boat deck. Four genoa and four mainsail trims were tested, resulting in 16 test conditions. The geometry of the sails and the pressure coefficients along four horizontal sections of each sail are provided herein. The predicted pressures from a vortex lattice method numerical code for the various sail test configuration were compared against the experimental data to verify the capability of the present database of providing a valuable benchmark. There was generally good agreement between the computed and measured pressures. The differences can mainly be explained by the action of viscosity. For example the numerical code could not model a leading edge separation bubble that occurred for some of the "tight" trims, and so the computations gave high leading edge suctions, and moved the second suction peak forward compared to the measured pressures.

1. INTRODUCTION

Sail aerodynamics is commonly investigated using wind tunnel tests or numerical codes. Two different sails can be tested in the same conditions to find the sail which develops the maximum driving force, or two sails can be tested in several different conditions to select the range over which one sail performs better than the other one or, finally, one sail can be tested to measure the aerodynamic forces to be used in a Velocity Prediction Program (VPP). In every case, the optimum sail trim, which maximises the drive force or the boat speed, has to be found. The greatest advantage of wind tunnel tests over numerical codes is the way in which the optimum trim is found. In fact, in wind tunnel tests, model-scale sails are trimmed remotely and the aerodynamic forces are displayed to the operator in real-time. When the optimum trim is achieved, the aerodynamic forces are measured with a balance attached to the model.

Numerical codes compute the optimum trim with arguably more difficulty, because the fluid dynamic code has to be coupled to a structural code. Several geometries have to be tested by the fluid dynamic code, which is time consuming if a viscous Navier-Stokes code is used.

While the flow is mainly attached on upwind sails (mainsails, jibs and genoas), a significant amount of separated flow occurs on downwind sails (spinnakers and gennakers). To correctly predict the aerodynamic forces from downwind sails, laminar to turbulent transition, reattachment and trailing edge separation have to be properly modelled [1]. Therefore, viscous Navier-Stokes codes must be used. Conversely, upwind sails can be adequately investigated with inviscid codes, such as the vortex lattice method.

It is common practice to couple inviscid fluid dynamic codes with finite element method (FEM) solvers. Inviscid codes allow several geometries to be processed very quickly. The computation of the aerodynamic forces can then be integrated into a VPP or into an optimisation program. Therefore, nowadays, inviscid numerical codes for sails are often developed for these purposes [2, 3, 4, 5].

The experimental validation of viscous and non-viscous codes is of great importance to the sail designer. It is common practice to use global aerodynamic forces to validate numerical codes, whereas, pressures on sails are rarely measured. As far as is known to the present authors, pressure distributions on three-dimensional upwind model-scale sails have never been published. Pressure distributions on full-scale sails were measured for the first time in 1925 by Warner & Ober [6], then by Puddu et al. [7], Graves et al. [8], and more recently by Viola & Flay [9] in 2010.

The present paper aims to provide a wide database of geometries and pressure distributions to validate both viscous and non-viscous codes in upwind sailing conditions. Upwind sails were tested in uniform flow without any supporting rigging (mast, boom, etc.). A flat plate was used to model the boat deck. Four genoa and four mainsail trims were tested, resulting in 16 test conditions. An inviscid numerical code was developed and tested against the experimental results. The experimental method is presented in Section 2, while the numerical method is presented in Section 3. The measured and the computed pressure distributions are discussed in Section 4. The geometries and an electronic copy of the presented results can be downloaded from www.ignazioviola.com or by emailing the corresponding author (im.viola@auckland.ac.nz).

2. EXPERIMENTAL METHOD

2.1 RIGID PRESSURE-TAPPED SAILS

A 1/15th model-scale rigid mainsail and genoa, originally designed by North Sails (New Zealand) Ltd. for the then proposed America's Cup class "AC33", were built and tested in the wind tunnel at Yacht Research Unit (YRU), University of Auckland (Figure 1 and 2). The sails were made of fibreglass and epoxy resin with a sandwich structure. The extruded polypropylene core resulted in parallel square tubes. The resulting sails were less than 4mm thick. Additional details describing the sail construction can be found in [10]. Several holes (pressure taps) were made along 4 horizontal sections of both the sails to enable the surface pressures to be measured at those locations. The pressures were transmitted to the sail foot through the vertical square core tubes. 1.5 mm bore PVC tubing was used to transmit the pressures from the sail foot to the pressure transducers.

2.2 WIND TUNNEL SETUP

The two sails were supported by tensioned thin nylon fishing line, which was almost transparent to the wind. Figure 2 shows the two sails during the wind tunnel test. A thin flat square plate was used to model the boat deck. The plate was 2440 mm wide, 9 mm thick and rotated 19° with respect to the wind tunnel axis in order to line up with the boat heading. The plate was positioned 600 mm above the wind tunnel floor, and thus above the wind tunnel floor boundary layer, which was about 200 mm high. There was no gap between the genoa foot and the plate. A hole in the plate allowed the pressure tubes to reach the transducers located below it. The pressure tubes from the mainsail were taped together to prevent the gap between the mainsail and the plate being blocked (Figure 3).

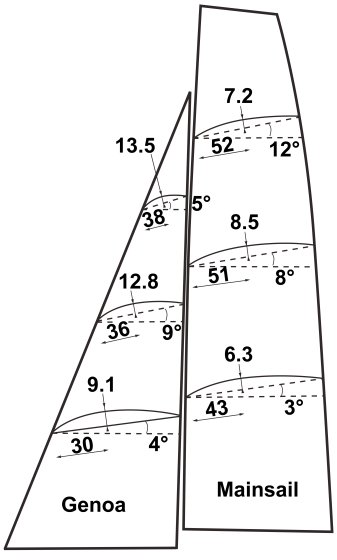

Figure 1: Draft, camber and twist of the two sails (in percentage of the chord length and degree respectively)

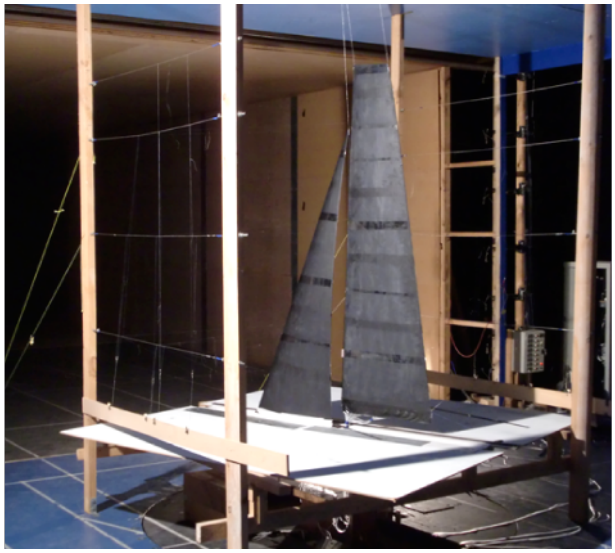

Figure 2: Photograph of the pressure-tapped sails mounted in the wind tunnel ready for testing.

2.3 PRESSURE MEASUREMENTS

The pressure transducers used in this research had a range of ±450 Pa and a resolution of 9.25 mV/Pa with an accuracy better than ±0.5 Pa. All the transducers were pneumatically connected to a reference static pressure p_∞, which was provided by the static tap of a Pitot-static tube located approximately 14 m upstream of the sails. Additional details of the pressure system are provided in [9].

The pressure measurements were initially acquired at 1,000 Hz for 5 minutes. Subsequent analysis of those data showed that high frequency signals were damped by the long tubes (up to 3m long) and hence, the sampling frequency was reduced to 100 Hz to reduce the amount of stored data. It was also found that a recording duration of 90 seconds contained several periods of the lowest frequency fluctuations and hence, the subsequent data acquisitions were performed for 90 seconds.

2.4 BOUNDARY CONDITIONS

The YRU wind tunnel has an open jet with a test section 7 m wide and 3.5 m high. The tunnel sidewalls stop 3.5 m upstream of the model location, while the roof and floor stop 2.1 m and 3.4 m downstream of the model location respectively. The top of the mainsail was 655 mm from the wind tunnel roof, which therefore is expected to have a negligible effect on the sail pressure distribution.

The tests were performed in uniform flow. The dynamic pressure was measured in empty wind-tunnel conditions at several locations. In the model region the mean dynamic pressure was q_∞=32.5 Pa with a variation of ±1 Pa for all the tests. The free-stream turbulence

intensity was about 3%. The Reynolds number *Re,* based on the average chord length c=0.49 m, was $Re=2.3\cdot10^5$.

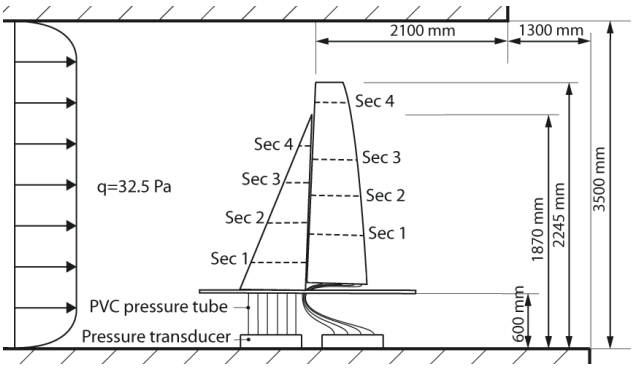

Figure 3: Schematic diagram showing the wind tunnel setup.

2.5 TEST CONDITIONS

The sails were tested upright (zero heel angle) at a yaw angle of 19°, defined as the supplementary angle in the horizontal plane between the free-stream velocity and the line through the tacks of the mainsail and the genoa.

Several sail trims were measured in previous tests [11], performed with the same sails fixed on a model-scale boat (instead of supported by fishing line). Those tests allowed the pressures and aerodynamic forces to be measured simultaneously. The optimum genoa and mainsail trims that gave the maximum drive force were measured. In the present paper, those previously determined optimum trims were replicated by suspending the sails with fishing line, without a hull in place. For each sail, three additional trims were tested. These trims were achieved by rotating the sail around its own luff. Thus, four genoa trims and four mainsail trims were tested, resulting in 16 test conditions. The sail twist did not change with the trim, as the sails were semi-rigid. For each sail, the trims are numbered from 1 to 4 in the figures, where 1 is the tightest trim and 4 the most eased trim. For instance, the optimum trim of the genoa is the 3rd tightest trim (named G3) while the optimum mainsail trim is the 2nd tightest trim (named M2).

In separate tests, several twist variations of the optimum trim (G3M2) were tested. In particular, 5 twists of each sail were tested. The results of these additional tests are not presented in the present paper but are available on the website mentioned above or by emailing the corresponding author. The effect of the mast and the boat hull on the resulting pressure distributions was also investigated and is discussed in [10].

2.6 TEST PROCEDURE

The pressure distribution on thin airfoils is very sensitive to the angle of attack (AoA). Sails are normally trimmed close to the ideal AoA, where the flow at the leading edge is tangent to the sail. Small deviations from this AoA can lead to significantly different pressure distributions at the leading edge. The maximum suction was measured at the leading edge of the genoa. This is because the upwash of the mainsail on the genoa leads to a higher AoA on the genoa, and furthermore the leach of the genoa is in a low pressure high speed area of flow around the mainsail, and this effect lowers the pressure over the entire genoa. Therefore to minimise the genoa trim variations, the genoa trim was modified after every 4 successive mainsail trims. For that reason, the trends in pressure distributions for different mainsail trims are more consistent than the trends in pressure for different genoa trims. For instance, when the pressure distributions measured with genoa trim G1, and mainsail trims from M1 to M4 are compared, the pressure trend is obtained with 4 successive data acquisitions. Conversely, the pressure distributions shown with mainsail trim M1 and genoa trims G1 to G4 were obtained after re-positioning the mainsail for each acquisition. Thus if the mainsail was not re-positioned in exactly the same place, a slightly different pressure distribution would result, and this might blur the underlying trend.

3. VORTEX LATTICE METHOD

To verify the capability of the present database to provide suitable benchmarks for numerical codes, all the test conditions were modelled with a numerical code based on the Vortex Lattice Method (VLM). The code has been based on the work of Werner, 2001 [12], but has undergone extensive revision. The present paper shows results from modeling each sail with 29 by 29 panels. Control points are positioned at the centre of each panel. Full-cosine spacing of the panels is used in both the chord-wise and span-wise directions. The wake is straight and aligned with the undisturbed free-stream direction. A mirror image of the sail is used to model the influence of the boat deck. No corrections are applied to take into account the viscous drag.

4. RESULTS

The pressure p measured by each pressure tap is presented in terms of a pressure coefficient Cp, defined as $Cp=(p-p_\infty)/q_\infty$. Note that reference values of the static and dynamic pressures were measured by the Pitot-static probe upwind of the model, and a pre-run calibration (without the sails in the wind tunnel) was done to determine the corrections required to determine the equivalent free-stream undisturbed values p_∞ and q_∞ at the model location.

4.1 CP ON THE GENOA FOR DIFFERENT MAINSAIL TRIMS

Figure 4 to Figure 8 present Cp versus the chord-wise position (x/c) for the genoa trims G1 to G4. Each figure shows 4 graphs for the 4 genoa sections (left) and 4 graphs for the 4 mainsail sections (right). The windward and the leeward Cps are both presented.

The top left graph of Figure 4 shows the *Cps* on the top genoa section (section 4), for the genoa trim G1 and the mainsail trims from M1 to M4. Note that the aeronautical convention of reversing the *Cp* axis has been adopted. On the suction side, the pressure shows an increasing trend from about *Cp*=-3.5 to about *Cp*= -1. The high suction on the forward part of the section shows that the genoa is trimmed at high AoAs. The second suction peak around x/c=30% is due to the section curvature.

The high adverse (positive) pressure gradient at the leading edge (downstream of the suction peak) causes the flow to separate and a leading edge bubble occurs. Laminar to turbulent transition occurs in the fore part of the bubble. The reattachment position is a stagnation point and hence, the velocity decreases and the pressure increases. If the flow were inviscid, separation will not occur and the pressure recovery would occur further upstream than in this real viscous flow. By easing the mainsail trim (from M1 to M4), the upwash from the mainsail onto the genoa is decreased and hence, the AoA on the genoa sections decreases. The lower the AoA, the more the *Cp* tends to zero on both sides of the sail.

On the windward side, the lower the AoA, the more downstream of the stagnation point the flow accelerates. At high AoA, the acceleration is small and *Cp* is almost 1 in the forward part of the sail section. The sail curvature can lead the *Cp* to increase up to x/c≈30% (for instance, section 4 in Figure 4). In the rear part of the sail section the pressure decreases up to the trailing edge.

On the leeward side of section 3 of the genoa, the pressure decreases from the leading edge to x/c≈30%, where the maximum camber is located. The absence of a leading edge suction peak here means that the section is trimmed near the ideal AoA.

On the leeward side of section 2 of the genoa, the pressures show different trends for different mainsail trims. When the mainsail is tightened to the maximum trim (M1), the high upwash leads to both a leading edge suction peak and a curvature-related suction peak. When the mainsail is eased (M2 to M4), the lower upwash leads to only a curvature related suction peak occurring.

On section 1 of the genoa, the *Cp* trends show some irregularities, which are possibly due to imperfections on the sail surface. The high AoA trim leads to a high leading edge suction followed by a strong positive pressure gradient. This adverse pressure gradient can lead to stall occurring. If stall had occurred, the pressure gradient would become almost zero. However, the measured pressure increases up to the trailing edge showing that there is a significant mean flow velocity gradient along the chord and hence, stall has not occurred.

4.2 CP AT THE LEADING AND TRAILING EDGES

It was not possible to measure the pressures right at the leading and trailing edges. The closest tap to the leading edge was at x/c=3, while the closest tap to the trailing edge was at x/c=97%.

If the flow were inviscid and the AoA were higher than the ideal AoA, the stagnation point would be on the windward side and *Cp* would tend towards -∞ at the leading edge on the leeward side. In viscous flow, the stagnation point is at the leading edge for a wide range of AoAs around the ideal AoA [9, 11]. Therefore, *Cp* is about 1 at the leading edge. If there was a significant cross flow occurring near the leading edge, then *Cp* would be slightly lower than 1.

The trailing edge pressure coefficient is negative on both the sails. In particular, it is lower on the genoa than on the mainsail because the trailing edge of the genoa is in the suction region of the mainsail [14]. The trailing edge pressure is lower on the sections nearest to the sail tips compared to the sections at mid-sail height. If the flow were inviscid, then the *Cp* would be zero at the trailing edge.

4.3 CP ON THE GENOA FOR DIFFERENT GENOA TRIMS

When the genoa is eased (from Figure 5 to 7), the AoA on every genoa section decreases. When the genoa is eased to the maximum setting (Figure 7), leading edge suction is absent on the leeward side, and the curvature-related suction decreases. On the windward side downstream of the stagnation point, the flow accelerates and the pressure reduces. The lower the AoA, the further downstream the minimum pressure occurs. When the AoA is lower than the ideal AoA, the flow separates at the leading edge and a leading edge bubble occurs on the windward side.

4.4 CP ON THE MAINSAIL AT DIFFERENT MAINSAIL TRIMS

In order to provide a simplified benchmark to validate numerical codes, the following results have been measured without the mast and the hull. The resulting mainsail had a thin profile with a sharp leading edge and hence the mainsail pressure distributions presented herein have much similarity to the genoa pressure distributions. In the following discussion, the main differences between the pressure distributions on the genoa and mainsail are commented upon.

The mainsail is affected by the downwash of the genoa, which leads to lower AoAs. Moreover, the mainsail is less cambered than the genoa and hence, the curvature-related suction is lower. Therefore, while the *Cps* on the leeward side of the genoa are approximately *Cp*=-2, on

the leeward side of the mainsail they are approximately *Cp*=-1.

It can be seen that on the leeward side of the mainsail, for every genoa trim (figures 4 to 7), when the mainsail is tightened to the maximum trim (M1) the *Cp* shows both a leading edge suction peak, which is due to the high AoA, and a curvature-related suction peak around x/c=30%. However when the mainsail is eased, the leading edge suction peak is absent and the curvature-related suction peak decreases.

The top mainsail section (section 4) is above the head of the genoa. Therefore, the downwash due to the genoa has much less effect on the top section, and compared to the lower sections the resulting AoA is therefore higher. When the mainsail is eased to the minimum trim (M4), the pressure on the leeward side shows that the leading edge suction is followed by a strong pressure recovery, which leads to trailing edge separation. In the separated region, the mean flow velocity and the velocity gradients are small and hence, the pressure gradient is almost zero. When the mainsail is tightened to the maximum trim (M1), the separation bubble at the leading edge does not reattach and stall occurs on the highest section of the mainsail. Therefore, the *Cp* distribution shows rather low gradients. For angles larger than the stall angle, the larger the AoA, the more *Cp* tends towards -1 over much of the leeward side of the sail.

It is known that the presence of the mast significantly affects the mainsail pressure distributions [15], and so the effects of the mast and hull on the resulting pressure distributions were investigated in the present research programme. The flat plate was moved down to model the water-plane, the hull was added between the sails and the plate and the mast was added in front of the mainsail. It was found that the presence of the mast leads to a significant reduction in the leeward-side leading-edge suction on the mainsail. The lift on the mainsail decreased of about 7% when tested in the presence of the mast and the hull. While the aerodynamic forces from the sails for real design cases must be computed taking by into account the mast and the hull, the present results show that for a preliminary design, the simpler approach of can be the two sails alone can be used to improve the design.

4.5 NUMERICAL/EXPERIMENTAL COMPARISON

Figure 8 shows the measured results compared with computed results using the VLM described earlier. It can be seen that the computed *Cps* are in good agreement with the experimental *Cps*, but some dissimilarities occur due to the inability of the code to compute viscous effects. For instance referring to the comparison between the VLM code and the experimental data for the optimum trim (G3M2), it is evident that because the VLM code does not take into account viscous effects, the stagnation point is at the leading edge for the ideal AoA only. For AoAs larger than the ideal AoA, the stagnation point is on the windward side. Therefore, if an infinite number of panels were used, the computed *Cp* would tend towards -∞ at the leading edge. On the windward side, *Cp*=1 at the stagnation point which occurs downstream of the leading edge.

At the ideal AoA, the computed *Cp* would tend towards 1 at the leading edge on both the leeward and windward sides. The numerical/experimental comparison shows that sometimes the measured *Cps* show only the curvature related suction peak even when the AoA is larger than the ideal AoA. For instance, on the top genoa section (section 4), the pressure recovery downstream of the leading edge suction peak was computed to be at x/c=3% and hence the leading edge suction peak was not able to be measured by the closest tap to the leading edge, which was at x/c=9%, well downstream.

On the leeward side, the minimum suction (between the two suction peaks) is computed to be at around x/c=5%, whereas it was measured to be at around x/c=15%. As mentioned above, the latter pressure recovery is caused by the leading edge bubble, which is not modelled by the numerical code. The maximum curvature-related suction is correctly computed. On the windward side, the pressure is slightly overestimated by the VLM, which is possibly related to the span-wise velocity due to the tip vortices.

On the top mainsail section (section 4), where the flow is mainly separated, the agreement between the inviscid code and the experimental data is poor, as expected. Conversely, on the lower sections where there is mainly little or no separation, the numerical and the experimental *Cps* are in good agreement.

5. CONCLUSIONS

In the present paper, a database of measured pressure coefficients to validate numerical CFD codes for upwind sailing conditions is provided. In the experiments, the geometry was simplified to the two sails alone, which were tested into the wind tunnel using wind-transparent supports. Pressure measurements were made along four horizontal sections of each of the rigid pressure-tapped sails. Four genoa trims and four mainsail trims were tested, resulting in 16 test conditions.

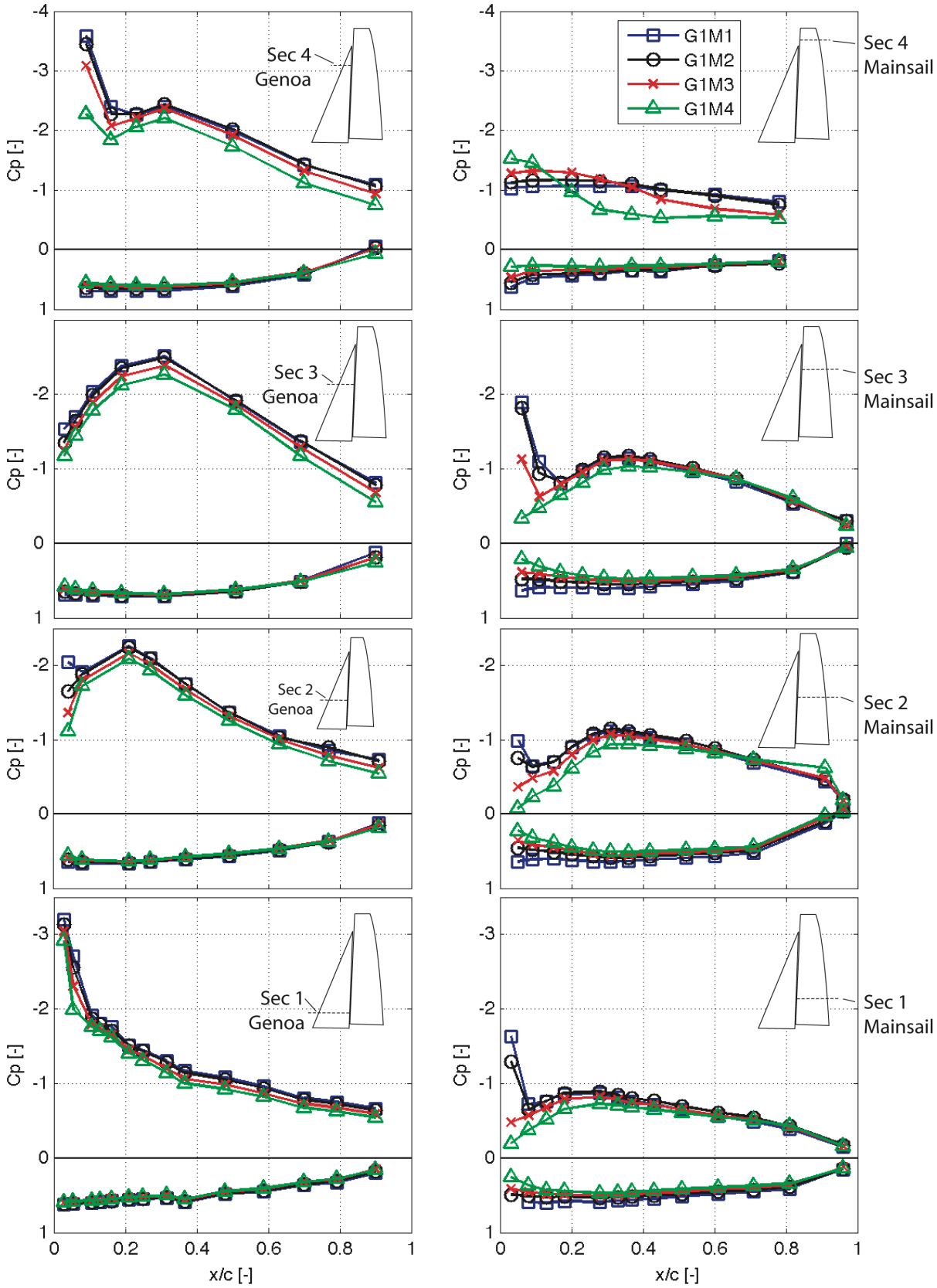

Figure 4: *Cp* on the genoa and the mainsail for the genoa trim G1 and all the mainsail trims (M1, M2, M3 and M4)

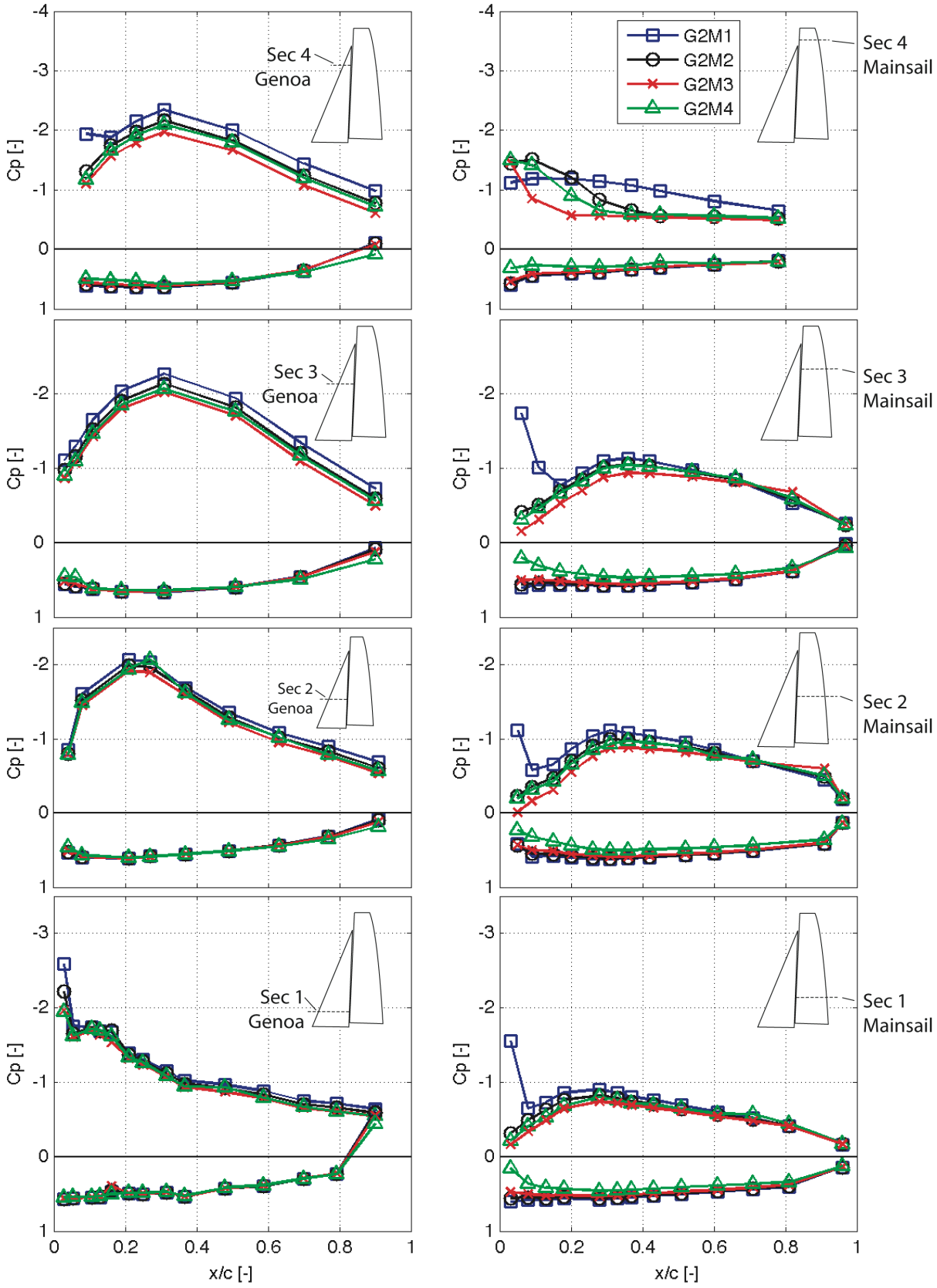

Figure 5: *Cp* on the genoa and the mainsail for the genoa trim G2 and all the mainsail trims (M1, M2, M3 and M4)

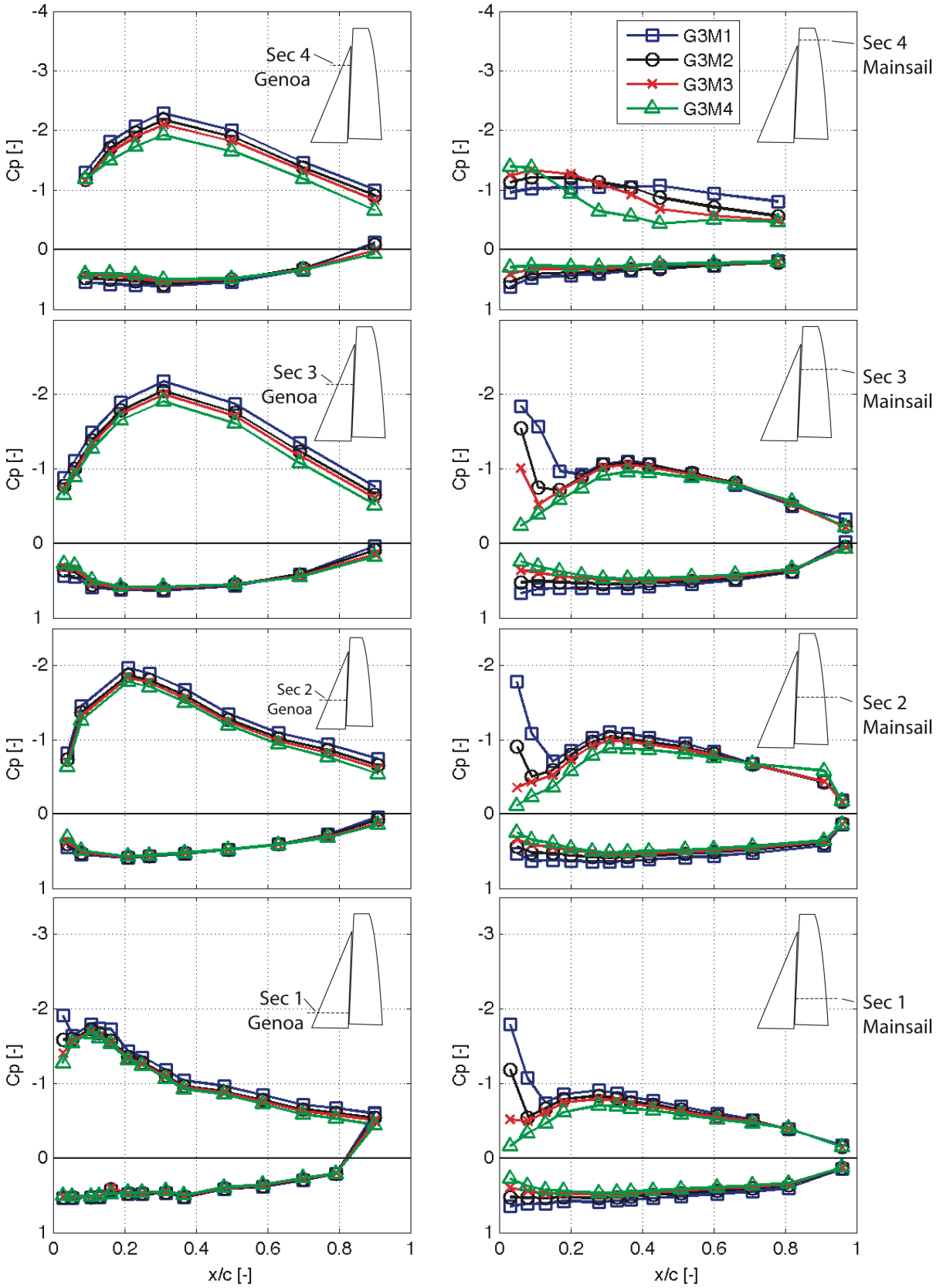

Figure 6: *Cp* on the genoa and the mainsail for the genoa trim G3 and all the mainsail trims (M1, M2, M3 and M4)

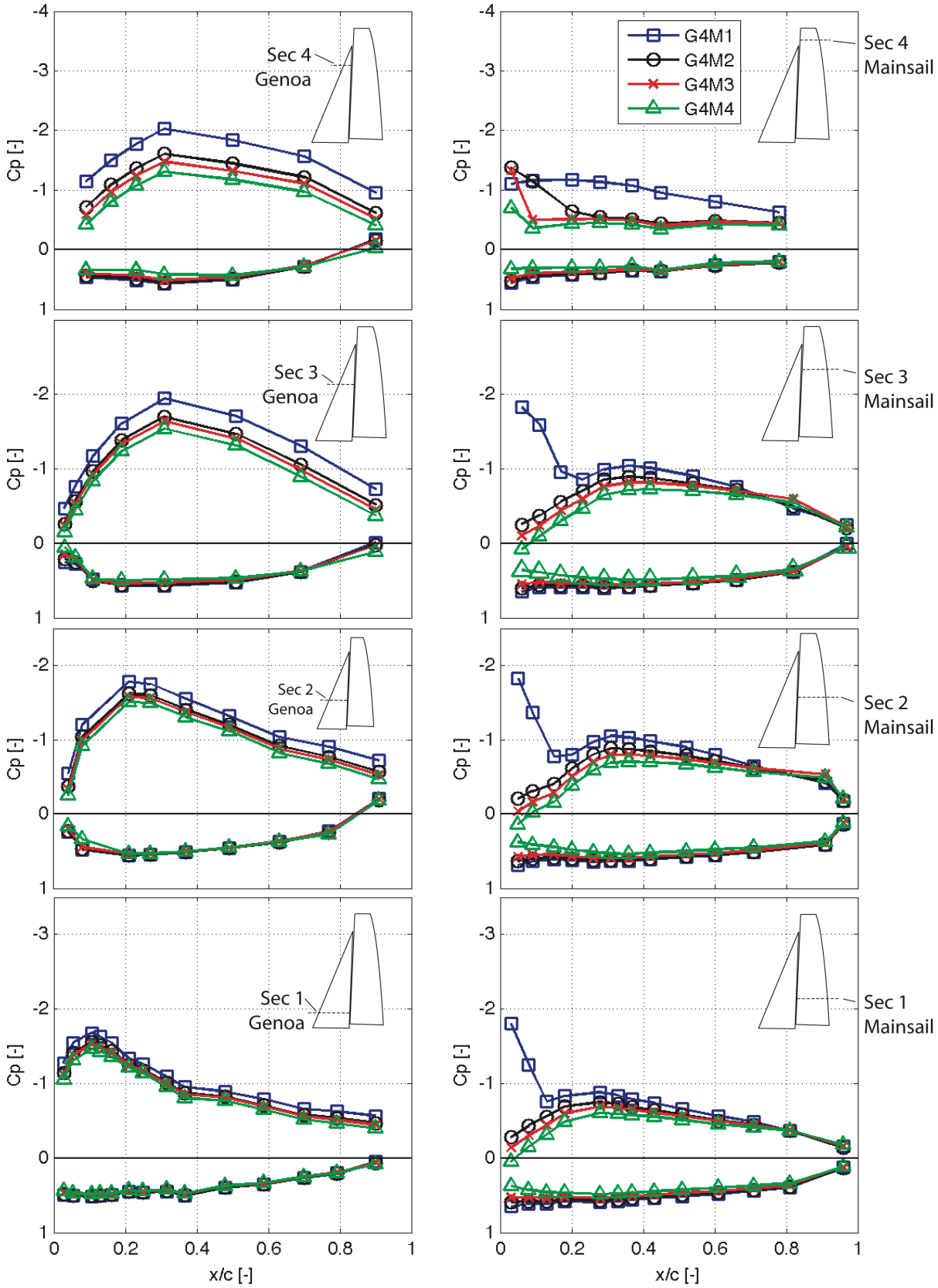

Figure 7: *Cp* on the genoa and the mainsail for the genoa trim G4 and all the mainsail trims (M1, M2, M3 and M4)

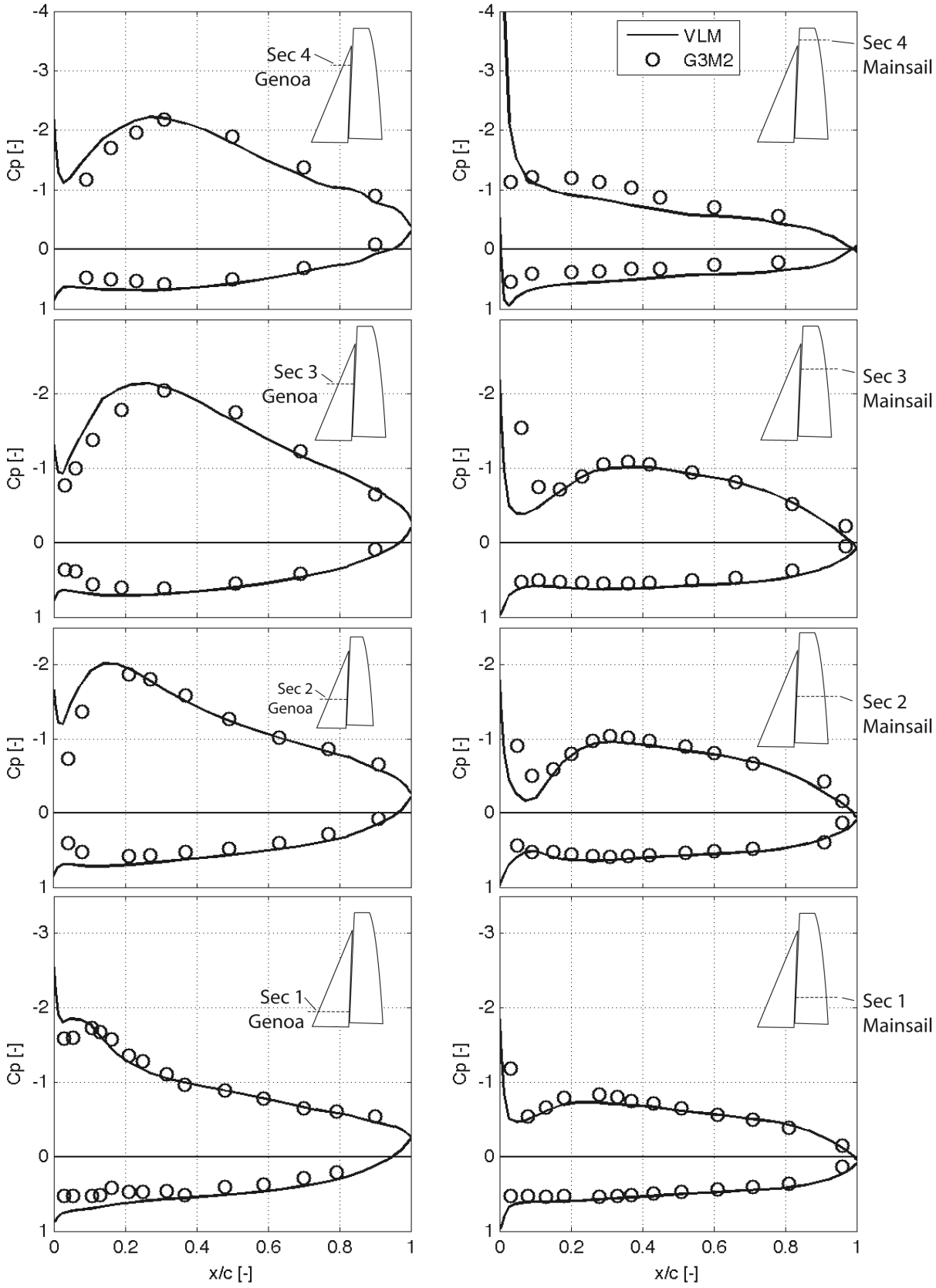

Figure 8: Numerical and experimental *Cp* on the genoa and the mainsail for the optimum trim (G2M3)

The measured pressure trends can be explained in terms of conventional aerodynamic theory for thin aerofoils. It was found that the pressure trends can be explained by the resulting angle of attack on each sail section. In the experiment, the sails have been trimmed to for angles of attack equal to or slightly higher than the ideal angle of attack. At the ideal angle of attack, only the curvature-related suction peak occurs on the leeward side, and there is no leading edge suction peak. At higher angles of attack, a leading edge bubble occurs and a suction peak occurs upstream of the curvature-related suction peak. The leeward suction pressure coefficients are higher for the genoa than for the mainsail. On the windward side, the pressure distribution showed significantly lower gradients, and the pressure coefficients are approximately 0.5 for most of the chord length.

A Vortex Lattice code used to predict the pressure distributions using the sail geometry data to check that the present database was capable of providing a valuable benchmark. In general good agreement was found between the numerical and the experimental data, but some differences were also found. In particular, on the leeward side, the minimum suction pressure between the two suction peaks was computed to be closer to the leading edge than obtained in the experimental measurements. This is due to the leading edge separation bubble that is neglected by the inviscid code. Poor agreement was found between the numerical and experimental results in the pressure distributions on the top section of the mainsail, which experiences higher angles of attack than the lower sections. This disagreement is due to the separation of the flow on this section, which can not be modelled by the inviscid VLM code.

6. ACKNOWLEDGEMENTS

The authors are very grateful to the numerous YRU students who were involved in the project and, in particular, to Mr. Manuel Fluck and Mr. Kurt McQuoid who built the sails and were involved in the wind tunnel testing. The support of the YRU, especially Frederik Gerhardt, is gratefully acknowledged.

7. REFERENCES

1. Viola I.M. and Flay R.G.J., Pressure Distribution on Modern Asymmetric Spinnakers, *International Journal of Small Craft Technology, Trans. RINA, vol. 152, part B1, pp. 41-50,* (DOI 10.3940/rina.ijsct.2010.b1.103) 2010.

2. Jackson P.S., The Analysis of Three-Dimensional Sails, *in the proceedings of the 10th Canadian Congress of Applied Mechanics, The University of Western Ontario, Canada, USA, pp. 59-67,* 1985.

3. Johnston M.S., An Aeroelastic Model for the Analysis of Membrane Wings, *PhD thesis, The University of Auckland, New Zealand,* 1997.

4. Ranzenbach R. and Xu Z., Sail Aero-Structures: Studying Primary Load Paths and Distortion, *In the proceedings of the 17th Chesapeake Sailing Yacht Symposium, Annapolis, USA, pp. 193-204,* 4-5 March 2005.

5. Malpede S. and Baraldi A., A fully Integrated Method for Optimizing Fiber-Membrane Sails, *In the proceedings of the 3rd High Performance Yacht Design Conference, Auckland, New Zealand, pp. 47-56,* 2-4 December 2008.

6. Warner E.P. & Ober S., The aerodynamics of Yacht Sails, *In the proceedings of the 3rd General Meeting of the Society of Naval Architects and Marine Engineers, vol. 33, pp. 207-232, New York, USA,* 12-13 November 1925.

7. Puddu P., Erriu N., Nurzia F., Pistidda A., Mura A., Full Scale Investigation of One-Design Class Catamaran Sails, *In the proceedings of the 2nd High Performance Yacht Design Conference, Auckland, New Zealand, pp. 131-136,* 14-16 February 2006.

8. Graves W., Barbera T., Braun J.B. Imas L., Measurement and Simulation of Pressure Distribution on Full Size Sails, *In the proceedings of the 3rd High Performance Yacht Design Conference, Auckland, New Zealand, pp. 239-246,* 2-4 December 2008.

9. Viola I.M. & Flay R.G.J., Full-scale Pressure Measurements on a Sparkman & Stephens 24-foot Sailing Yacht, *Journal of Wind Engineering and Industrial Aerodynamics*, in press.

10. Fluck M., Gerhardt F.C., Pilate J. and Flay R.G.J., Comparison of Potential Flow Based and Measured Pressure Distributions Over Upwind Sails, *Journal of Aircraft,* in press.

11. Viola I.M. and Flay R.G.J., Pressure Measurements on Full-Scale and Model-Scale Upwind Sails, *In the proceedings of the 17th Australasian Fluid Mechanics Conference, Auckland, New Zealand,* 5-9 December 2010.

12. Werner S., Application of the Vortex Lattice Method to Yacht Sails, *Master of Science Thesis, Department of Mechanical Engineering, Technical University of Denmark,* July 2001.

13. Crompton M.J. and Barret R.V., Investigation of the Separation Bubble Formed Behind the Sharp Leading Edge of a Flat Plate at Incidence, *In the proceedings of the Institution of Mechanical Engineers, Part G: Journal*

of Aerospace Engineering (ISSN 0954-4100), Vol. 214, (3), pp. 157-176, 2000.

14. Gentry A., The Aerodynamics of Sail Interaction, *In the proceedings of the 3rd AIAA Symposium on the Aero/Hydronautics of Sailing, Redondo Beach, California, USA,* 20 November 1971.

15. Wilkinson S., Partially Separated Flows Around 2D Masts and Sails, *PhD Thesis, University of Southampton, England,* August 1984.